ARMA 10-380

SAND2010-1529C

Sensitivity of Storage Field Performance to Geologic and Cavern Design Parameters in Salt Domes

Park, B. Y. and Ehgartner, B.L.
Sandia National Laboratories, Albuquerque, NM, USA
Herrick, C.G.
Sandia National Laboratories, Carlsbad, NM, USA

This paper was prepared for presentation at the 44th US Rock Mechanics Symposium and 5th U.S.-Canada Rock Mechanics Symposium, held in Salt Lake City, UT June 27–30, 2010.

ABSTRACT: A sensitivity study was performed utilizing a three dimensional finite element model to assess allowable cavern field sizes in strategic petroleum reserve salt domes. A potential exists for tensile fracturing and dilatancy damage to salt that can compromise the integrity of a cavern field in situations where high extraction ratios exist. The effects of salt creep rate, depth of salt dome top, dome size, caprock thickness, elastic moduli of caprock and surrounding rock, lateral stress ratio of surrounding rock, cavern size, depth of cavern, and number of caverns are examined numerically. As a result, a correlation table between the parameters and the impact on the performance of storage field was established. In general, slower salt creep rates, deeper depth of salt dome top, larger elastic moduli of caprock and surrounding rock, and a smaller radius of cavern are better for structural performance of the salt dome.

1. INTRODUCTION

1.1. Background

Salt domes have served as excellent hosts for the storage of oil and gas in underground caverns. Because of the desire to expand their use, there are concerns about the integrity of the salt surrounding these storage caverns that need to be addressed. An actual example of a dome that experienced salt damage with a resulting loss of an underground oil storage capacity is the Weeks Island dome. Oil was stored in an abandoned room and pillar mine. A sinkhole developed as a result of salt cracks that formed along the top of the dome and penetrated into the mined facility. Finite element analyses predicted salt dilatant damage and tensile stresses to form as a result of subsidence over time [1]. In addition, a large amount of subsidence and volumetric change to the caverns due to salt creep closure was predicted and measured. It appears that salt domes have limits to the amount and/or rate of underground closure allowed.

Based on experience suggested from past numerical analyses [2, 3, 4, and 5], one area of concern is the possible loss of integrity to the salt above the caverns. Dilatant damage may develop over time in a small dome with fast creeping salt where damage may initiate at the top of the dome and extend downward with time to the roof of the cavern field. Another area of possible concern is the effect of the combination of numerous large deep caverns in a single dome. Again, this is especially important in a fast creeping salt.

1.2. Approach

The cavern field studied herein will be symmetric so that readily deployed pie-slice models can be used. The base model will be the 19 cavern field model used for our West Hackberry (WH) analysis [2]. The 30-degree wedge model will incorporate a dome edge appropriate for the site. Periodic workovers will be simulated, but progressive leaches of the caverns for the drawdowns will not be considered. Individual parameters will be varied from the base model to access their impact on the integrity of the salt. This will be accomplished by assessing the sensitivity of the predicted safety factor against damage to the individual parameter variations of interest.

1.3. Objectives

The goal is to establish conditions whereby cavern field integrity may be compromised. The contributing factors are to be identified and quantified relative to their impacts. The results may be generalized to define conditions for allowable underground closure relative to

dome size. If damage is predicted, then certain cavern field designs in combination with certain geologic conditions are unacceptable. These will need to be quantified.

1.4. Applications

The results from this study will be used for cavern design, dome selection, monitoring, and forecasting potential problems. While we have the latitude to vary design parameters to accommodate a specific dome, many times we also have the ability to select a particular dome. Therefore, the results of this study can aid in dome selection and design of a cavern field to suit a particular dome. For existing sites, this parametric study may foresee certain conditions that could become problematic as additional caverns are added to a field or existing ones enlarged.

2. PARAMETERS

Parameters of interest are those capable of leading to salt damage around the cavern field. As mentioned in Section 1.1, the most likely place for damage to be initiated is at the top of a salt dome. This damage may become extensive enough to propagate down through the salt and jeopardize the integrity of the caverns. Continued deformation and subsidence may result in crack propagation and/or dilation that extends into the storage areas. This situation appears to be associated with large volumetric closures of caverns in a small dome. Therefore, our suggested baseline model is a small dome in a relatively fast creeping salt formation. Individual parameters will be varied (one by one) from the baseline model to assess the impact on the integrity of the salt. This will establish the sensitivity of the predicted safety factor against damage to the individual parameter variations of interest. It will also constitute the initial scoping part of the study. If necessary and realistic, additional parameter sets can be selected dependent upon after review of the results. The specific modeling parameters used to examine their impacts on the salt dome damage are listed in Table 1 along with the typical base values and the variants. Note that the first seven items in the table are geologic parameters, which are characteristics of a site that cannot be changed, only measured. The final three parameters are design options. Figure 1 shows the denotation of each parameter in Table 1 on the mesh.

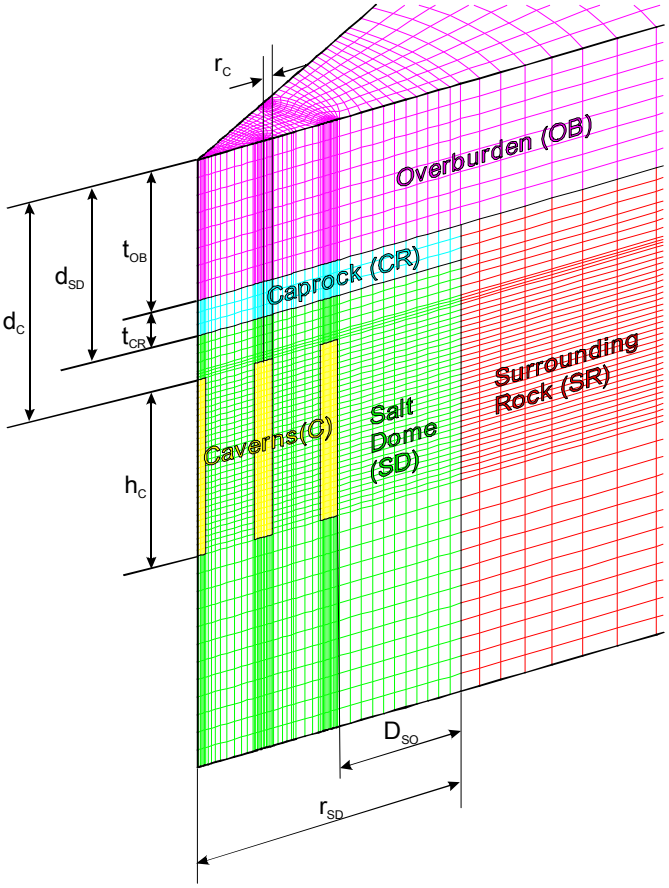

Figure 1. Denotation of each parameter in Table 1.

3. ANALYSIS MODEL

3.1. Salt Constitutive Model

The scalar secondary creep strain rate is determined from the following law:

$$\dot{\varepsilon} = A_{SC}\left(\frac{\bar{\sigma}}{\mu}\right)^{n} \exp\left(-\frac{Q}{RT}\right) \qquad (1)$$

where, $\dot{\varepsilon}$ = scalar secondary creep strain rate; $\bar{\sigma} = \sigma_1 - \sigma_3$ = Tresca equivalent stress; σ_1 = maximum principal stress; σ_3 = minimum principal stress; μ = elastic shear modulus = $E/2(1+\nu)$; E = elastic modulus; ν = Poisson's ratio; T = absolute temperature (K); A_{SC} = secondary creep constant (s^{-1}), n = stress exponent; Q = activation energy (cal/mole); and R = universal gas constant (cal/(mole·K)).

Table 1. The specific modeling parameters with the typical base values and its variant.

	Check Effect	Parameter	Baseline	Variant	Comment
Geologic Parameter	Salt Creep Rate	Secondary Creep Constant, A_{SC} (s^{-1})	$A_{SC} = 11\times10^{12}$	$A_{SC} = 5\times10^{11}$ and $A_{SC} = 2\times10^{14}$	n=5 and μ=12.4 GPa, Q=10,000 cal/mol†
	Top of Salt Dome Depth ($d_{SD} = t_{OB} + t_{CR}$)	Thickness (ft) of Overburden, t_{OB}, and Caprock, t_{CR}	t_{OB} = 1600 t_{CR} = 400 d_{SD} = 2000	t_{OB} = 100 t_{CR} = 400 d_{SD}= 500	Maintain 400 ft of caprock, reduce overburden to 100 ft
	Dome Size, Standoff Distance	Dome Radius, r_{SD} (ft)	r_{SD} = 3000	r_{SD} = 1700	From center of model
	Caprock Thickness	Caprock Thickness, t_{CR} (ft)	t_{OB} = 1600 t_{CR} = 400	t_{OB} = 400 t_{CR} = 1600	Reduce overburden thickness to 400 ft and increase caprock thickness to 1600 ft
	Elastic Modulus of Caprock	Modulus of Caprock, E_{CR} (GPa)	E_{CR} = 7	E_{CR} = 1, E_{CR} = 20, and E_{CR} = 100	Based on Hoffman and Ehgartner [6]
	Elastic Modulus of Surrounding Rock	Modulus of Rock, E_{SR} (GPa)	E_{SR} = 70	E_{SR} = 4, E_{SR} = 10, E_{SR} = 20, and E_{SR} = 30	High and low values are based on Richton data [7]
	Lateral Stress Ratio†† of Surrounding Rock	Coefficient of Rock, $\mathcal{K}_{SR}$	$\mathcal{K}_{SR}$ = 0.49	$\mathcal{K}_{SR}$ = 1, and $\mathcal{K}_{SR}$ = 2	Based on Lambe and Whitman [8]; Hoek and Brown [9]
Design Parameter	Cavern Size	Cavern Radius, r_C (ft)	r_C = 100	r_C = 200	Radius held constant with depth. Spacing of caverns is 750 ft
	Cavern Depth	Cavern Depth, d_C (ft)	d_C = 2500	d_C = 1000, d_C = 2100, and d_C = 4000	Cavern height (h_C) maintained at 2000 ft
	Number of Caverns	Number of Caverns, N_C	N_C = 19	N_C = 31	

†: variables in Eq. (2); ††: the ratio of the average horizontal to vertical stress.

To make the simulations more manageable, the transient creep effects were ignored and the steady state creep response was treated using the power law creep model in JAS3D[1]. In essence the transient creep in the early-time response was not represented in these simulations. The scalar secondary creep strain rate for the power law creep model in JAS3D is given by:

$$\dot{\varepsilon} = A\bar{\sigma}_{vm}^{n}\exp\left(-\frac{Q}{RT}\right) \tag{2}$$

where $A=$ power law creep constant (Pa^{-n}/s) and $\bar{\sigma}_{vm} = \sqrt{3J_2}$ = von Mises equivalent stress (Pa); J_2 = second invariant of the deviatoric stress tensor.

For the case of triaxial compression ($\sigma_1 = \sigma_2 > \sigma_3$, where σ_i are the principal stresses), the Tresca equivalent stress and the von Mises equivalent stress are equal. Equating the two equations for scalar secondary creep strain rate allows the determination of the creep constant, A, used in the power law creep model [10].

$$A = \frac{A_{SC}}{\mu^{n}} \tag{3}$$

[1] JAS3D is a Sandia National Laboratories 3-D FEM internal software package.

The values used as baseline input data in the present analyses are listed in Table 2.

Table 2. Material properties of salt for baseline analyses.

Parameter	Unit	Value	Reference
Young's modulus (E)	GPa	31	Krieg [11]
Density (ρ)	kg/m^3	2300	Krieg [11]
Poisson's ratio (ν)	-	0.25	Krieg [11]
Elastic modulus reduction factor (RF)	-	1.0	
Bulk modulus (K)	GPa	20.7	Computed from E and ν
Elastic shear modulus (μ)	GPa	12.4	Computed from E and ν
Stress exponent (n)	-	5.0	
Secondary creep constant (A_{SC})	s^{-1}	1.1×10^{13}	
Power law creep constant (A)	Pa^{-n}/s	3.75×10^{-38}	Computed from A_{SC}
Structure multiplication factor (SMF)	-	1.0	
Activation energy (Q)	cal/mol	10,000	
Universal gas constant (R)	cal/(mol·K)	1.987	-
Input thermal constant (Q/R)	K	5033	-
Lateral stress ratio ($\mathcal{K}$)	-	1.0	σ_h / σ_v

3.2. *Lithologies around the Salt Dome*

An elastic model is assumed for the lithologies encompassing the salt dome. The surface overburden layer is assumed to exhibit elastic material behavior. The overburden layer is considered isotropic and has no assumed failure criteria. The caprock layer is also assumed to behave elastically. The rock surrounding the salt dome is assumed isotropic, homogeneous elastic rock. The mechanical properties used in the baseline analysis are listed in Table 3.

Table 3. Material properties of lithologies around salt dome used in the analyses.

	Unit	Overburden	Caprock	Surrounding Rock
Young's modulus (E)	GPa	0.1	7.0	70
Density (ρ)	kg/m^3	1874	2500	2500
Poisson's ratio (ν)	-	0.33	0.29	0.33
Lateral stress ratio (κ)	-	0.49	0.41	0.49

3.3. *Cavern Geometry and Layout*

Symmetric 19-cavern field model at West Hackberry is used for the baseline model so that readily deployed pie-slice models can be used [2]. The 30-degree wedge model incorporates dome geometry appropriate for the site. Periodic workovers[2] are simulated, but progressive leaches of the caverns for the drawdowns[3] are not considered. Figure 2 shows a schematic of 19-cavern field layout and cavern rings considered during the periodic workovers. Figure 3 shows the computational mesh and boundary conditions used for the baseline calculation. Four material blocks are used in the model. They are overburden, caprock, salt dome, and the lithologies surrounding the salt dome.

The diameter of the caverns is 61 m (200 ft), the distance between caverns is 231 m (750 ft), the dome radius is 914 m (3000 ft), and the far-field boundary is 4572 m (15,000 ft) from the center of the dome. As listed in Table 1, the overburden thickness is 488 m (1600 ft), the caprock thickness is 122 m (400 ft), the depth of salt dome top is 610 m (2000 ft), and the depth of cavern top is 762 m (2500 ft).

3.4. *Model History*

This analysis simulates cavern leaching by gradually and systematically replacing the salt mesh regions of the cavern volume with fresh water regions over a one year construction period. At this point in time, the strategic petroleum reserve (SPR[4]) caverns were assumed to be filled with crude oil and then permitted to creep for 45 years. Leaching is assumed to occur uniformly along the entire height of the cavern. However, leaching is not permitted in the floor or the roof of the caverns. After the initial leach, all caverns in the array were periodically and systematically subjected to cavern workovers. The simulation was performed for a total of 46 years.

Both normal cavern operating conditions and workover conditions are simulated. For normal operating conditions, the cavern pressure is based on a wellhead pressure of 6.38 MPa (925 psi) caused by the fluid in the cavern at a depth of 762 m (2500 ft). For workover conditions, zero wellhead pressure is used. Workover durations are three months. For both normal and workover conditions, the caverns are assumed to be full of oil having a pressure gradient of 8370 Pa/m (0.37 psi/ft) of depth.

The schedule for workover is based on dividing the cavern array into "cavern rings" of constant radius. The numbered caverns shown in the 30° wedge section of Figure 2 each represent the caverns of that ring. The solution results for the representative cavern are identical for all of the caverns in a given ring. Thus, Cavern Ring 1 represents one cavern, Cavern Ring 2 represents six caverns, as does Cavern Ring 3 and Cavern Ring 4.

To better simulate actual field conditions, not all caverns are in workover mode at the same time. The central cavern in the field (Cavern 1 in Figure 2) is the first cavern in the workover sequence beginning one year after initial cavern leaching. It undergoes a workover every five years thereafter until the end of the simulations. The next closest neighboring cavern (Cavern 2 in Figure 2) is due to be worked over the following year. Because of mesh symmetry, this means workover pressures are applied to the six caverns that make up this second set of caverns, containing Cavern 2, at the same time. This results in the six caverns closest to Cavern 1 at low pressure beginning workover one year after workover of the central cavern. This condition enables the web of salt between adjacent caverns in workover mode to be examined for stability. In addition, the webs of salt between caverns in workover mode and those under normal operating pressures can be studied. The workover sequence continues with the outmost cavern along the 0° symmetry plane (Cavern 3 in Figure 2) being subject to workover pressures one year after the second set of caverns. The final set of caverns to

[2] "Workover" is when the wellhead pressure in the cavern is dropped to zero for maintenance.

[3] "Drawdown" is when the crude oil is withdrawn from the cavern. Fresh water is used to withdrawal the crude oil. Because the cavern enlarges due to salt dissolving from the cavern walls, it is called a "drawdown leach".

[4] The US SPR program currently stores 727 MMB of petroleum in 62 caverns located in four salt domes along the Gulf of Mexico.

undergo workover in the fifth year is that along 30° symmetry plane (Cavern 4 in Figure 2). This cycle is repeated every five years until the end of the simulations.

Figure 4 shows the wellhead pressure change in each cavern.

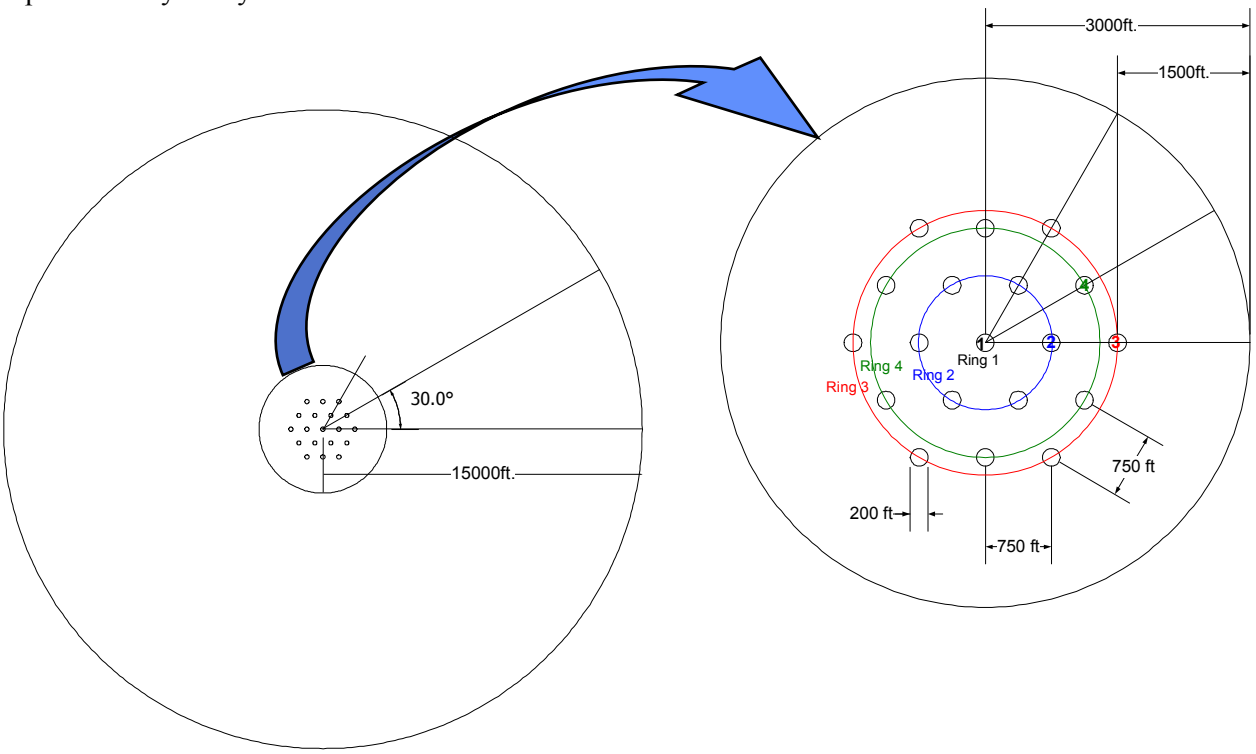

Figure 2. Schematic of 19-cavern field layout and cavern ring nomenclature.

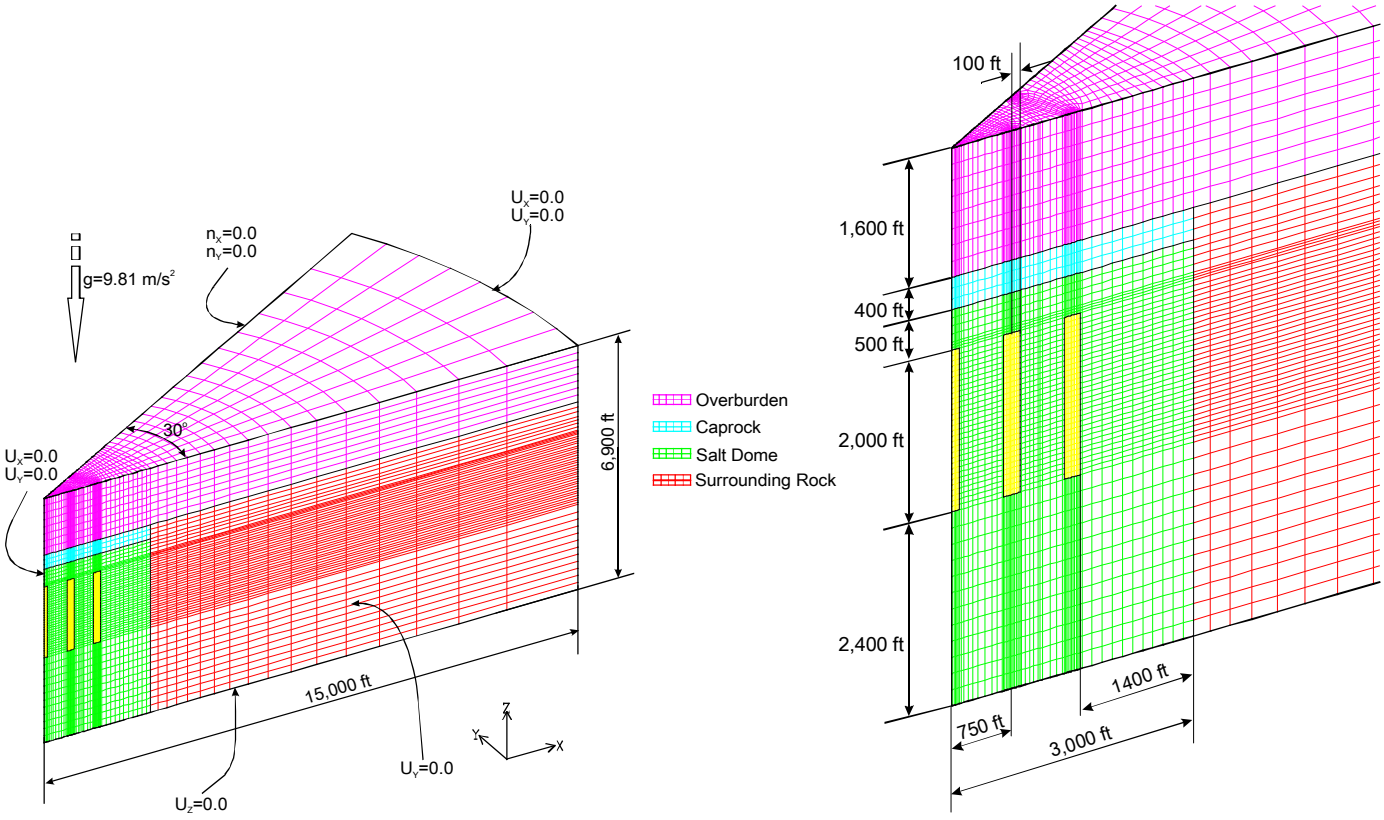

Figure 3. Computational mesh and boundary conditions of the baseline calculation.

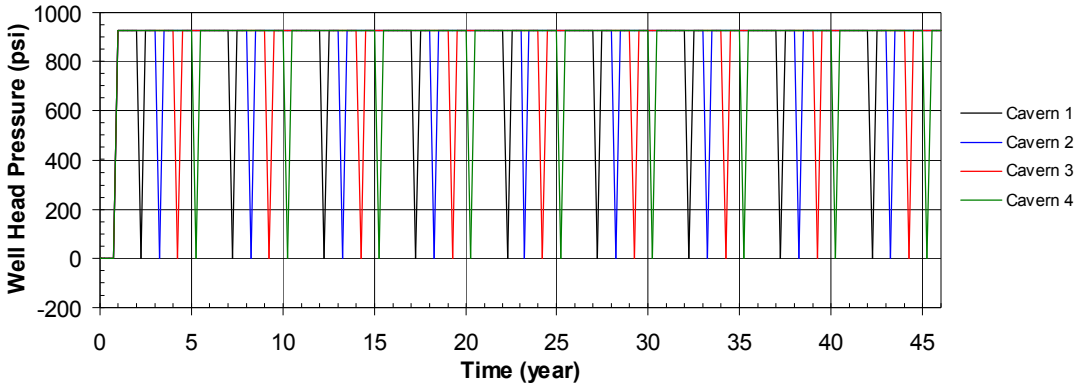

Figure 4. Wellhead pressure change in each SPR cavern.

3.5. Thermal Conditions

The finite element model includes a depth-dependent temperature gradient, which starts at 37.0°C (98.6°F) at the surface and increases at the rate of 1.95°C/100 m (0.0107°F/ft). The temperature profile is based on the average temperature data recorded in well logs from West Hackberry prior to leaching [12]. The temperature distribution is important because the creep response of the salt is temperature dependent. Radial temperature gradients due to cavern cooling effects from the cavern contents are not considered in these calculations. Previous 2D cavern studies have shown the predicted cavern deformation to be insensitive to the developed radial thermal gradients [6].

4. EFFECT OF EACH PARAMETER

A sensitivity study was performed utilizing a three dimension finite element model to assess the effect of various cavern field sizes for salt dome. Calculation details are documented in a report by Park and Ehgartner. [13].

4.1. Effect of Salt Creep Rate

To examine the salt creep rate effect, the analyses are conducted using secondary creep constants of $5\times10^{11}(s^{-1})$ and 2×10^{14} (s^{-1}) instead of 1.1×10^{13} (s^{-1}) for the baseline. The associated power law creep constants for the computer input data are calculated to be 1.71×10^{-39} (Pa^{-n}/s) and 6.82×10^{-37} (Pa^{-n}/s), respectively instead of 3.75×10^{-38} (Pa^{-n}/s). The mesh, model history, and thermal conditions are the same as those for the baseline case. All of the material properties except the creep constant for the salt dome are also the same as those for the baseline

Based on an interpretation of the analyses results, smaller values of the secondary creep constant are more advantageous from storage loss, subsidence, integrity of a surface structure, and cemented well annulus viewpoints. A smaller value of the creep constant does not always appear better from a tensile failure viewpoint. Until about 17 years, a larger value of the secondary creep constant is better from a dilatancy damage viewpoint. The optimum value of the constant against tensile failure and dilatancy exists between upper and lower bounding values of 2.0×10^{14} (s^{-1}), 5.0×10^{11} (s^{-1}), respectively.

4.2. Depth of Salt Dome Top Effect with Salt Creep Rate

To examine the depth effect of salt dome top, the mesh was modified so that the depth of salt dome top is 152 m (500 ft) instead of 610 m (2000 ft) for the baseline. The cavern depth is maintained at 762 m (2500 ft). The material properties for the salt dome, overburden, caprock, and surrounding rock are the same as those for the baseline case. The model history and thermal conditions are also the same as those for the baseline.

To examine the depth of salt dome top effect with faster salt creep rate, a secondary creep constant of 2×10^{14} (s^{-1}) instead of 1.1×10^{13} (s^{-1}) was applied on the modified mesh. The material properties for the fast creeping salt (FCS), based on a dome in the Gulf Coast, are also applied for examining with the actual lithologies. The FCS dome is located east of Galliano, LA in Lafourche Parish. All of the material properties except the creep constant for the salt dome are the same as those for the baseline. The model history and thermal conditions are also the same as those for the baseline. Table 4 lists the parameter values used for computer input to examine the depth of salt dome top effect. The blue bold fonts indicate the different values from the baseline.

Based on an interpretation of the analyses results, a deeper depth of the salt dome top is more advantageous from a storage loss, subsidence, integrity of a surface structure, cemented well annulus, and structural stability viewpoints. A smaller value of the secondary creep constant (slower creep rate) is more advantageous from a storage loss, subsidence, integrity of a surface structure, cemented well annulus, and structural stability viewpoint.

This is similar to the results in Section 4.1 even though the depth of the salt dome top is shallower.

Table 4. The parameter values used to examine the depth of salt dome top effect.

Parameter	Unit	Baseline d_{SD}=2000 A_{SC}=1.1×10^{13}	d_{SD}=500 A_{SC}=1.1×10^{13}	d_{SD}=500 FCS	d_{SD}=500 A_{SC}=2×10^{14}
Overburden Thickness (t_{OB})	ft	1600	**100**	**100**	**100**
Caprock Thickness (t_{CR})	ft	400	400	400	400
Depth of Salt Dome Top (d_{SD} = t_{OB} + t_{CR})	ft	2000	**500**	**500**	**500**
Depth of Caverns (d_C)	ft	2500	2500	2500	2500
Secondary Creep Constant (A_{SC})	s^{-1}	1.1×10^{13}	1.1×10^{13}	**2.26×10^{13}**	**2×10^{14}**
Power Law Creep Constant (A)	Pa^{-n}/s	3.75×10^{-38}	3.75×10^{-38}	**7.72×10^{-38}**	**6.82×10^{-37}**
Bulk modulus (K)	Pa	2.07×10^{10}	2.07×10^{10}	**3.41×10^{10}**	2.07×10^{10}
Two mu (2μ)	Pa	2.48×10^{10}	2.48×10^{10}	**1.94×10^{10}**	2.48×10^{10}

4.3. Effect of Dome Size and Standoff Distance

To examine the effect of dome size and standoff distance[5], the mesh was modified so that the radius of salt dome is 518 m (1700 ft) instead of 914 m (3000 ft) for the baseline case. The standoff distance from the edge of the outmost cavern to the edge of the dome is then 30 m (100 ft) instead of 427 m (1400 ft) for the baseline case. The material properties for the salt dome, overburden, caprock, and surrounding rock are the same as those for the baseline. The model history and thermal conditions are also the same as those for the baseline.

Upon an interpreting the analyses results, a smaller radius of salt dome is more advantageous from storage loss, subsidence, integrity of surface structures, and dilatant damage viewpoints. The radius of the salt dome has little effect on the structural stability against tensile failure. Smaller standoff distance from the edge of the outmost cavern to the dome edge is not better in terms of the vertical strain above the roof of the outmost cavern.

4.4. Effect of Caprock Thickness

To examine the effect of caprock thickness, the mesh of the baseline model was modified so that the caprock thickness is 488 m (1600 ft) instead of 122 m (400 ft) for the baseline. The depth of the salt dome top was maintained at 610 m (2000 ft). The overburden thickness was then 122 m (400 ft) instead of 488 m (1600 ft) for the baseline. The material properties for the salt dome, overburden, caprock, and surrounding rock are the same as those for the baseline. The model history and thermal conditions are also the same as those for the baseline.

After interpreting the results of the analyses, a larger thickness of caprock is more advantageous from a subsidence viewpoint. However, it is not better from storage loss and vertical strain above the roof of the caverns viewpoints. However, those impacts are not much in terms of the overall stability of the salt in the dome. The thickness of the caprock has a little effect on the radial surface strain and the structural stability against tensile failure and dilatant damage.

4.5. Elastic Modulus Effect of Caprock Rock

To examine the effect of the elastic modulus of the caprock, analyses were conducted using 1 GPa, 20 GPa, 100 GPa as the elastic moduli of caprock instead of 7 GPa for the baseline case. The baseline mesh shown in Figure 3 was used. The model history and thermal conditions are the same as those for the baseline. All of the material properties except the elastic modulus of caprock are also the same as those for the baseline.

From an interpretation of the analyses results, a larger value for the elastic modulus of the caprock is slightly more advantageous from a storage loss, subsidence, integrity of surface structures, and cemented well annulus perspective. The value of elastic modulus of the caprock does not affect the structural stability of the caverns when the value is larger than 7 GPa.

4.6. Surrounding Rock Elastic Modulus Effect

To examine the effect of the elastic modulus of the surrounding rock, analyses were conducted using 4 GPa, 10 GPa, 20 GPa and 30 GPa for the elastic moduli of surrounding rock instead of 70 GPa used in the baseline. The upper and lower bound values are derived from the Richton site data [7]. The baseline mesh was used. The model history and thermal conditions are the same as those for the baseline. All of the material properties except the elastic modulus of surrounding rock are also the same as those for the baseline.

Based on an interpretation of the analyses results, a smaller value for the elastic modulus of the surrounding rock is slightly more advantageous from a storage loss and stability of a cemented well annulus perspective. However, a larger value is more advantageous for the integrity of surface structures. The value of elastic modulus of the surrounding rock does not affect the structural stability of the caverns much when the value is larger than 10 GPa.

4.7. Surrounding Rock Lateral Stress Ratio Effect

The ratio of horizontal to vertical stress in subsurface is expressed by a factor called the *coefficient of lateral stress* or *lateral stress ratio* [8]. It is denoted by the symbol $\mathcal{K}$:

$$\mathcal{K} = \frac{\sigma_h}{\sigma_v} \tag{4}$$

where, σ_h = average horizontal stress; and σ_v = vertical stress [9].

[5] The distance between the wall of outmost cavern in the dome and the edge of the salt dome.

The lateral stress ratio of surrounding rock rather than the stresses due to the caprock and/or overburden may have large impact on the salt dome behavior because the dome is encircled by the surrounding rock. To examine the effect of the lateral stress ratio of the surrounding rock, analyses are conducted using $\mathcal{K}$ values of 1.0 and 2.0 instead of 0.49 as used in the baseline case. The baseline mesh was used. The model history and thermal conditions are the same as those for the baseline. All of the material properties except the lateral stress ratio of surrounding rock are the same as those for the baseline

Based on an interpretation of the analyses results, it was found that when the lateral stress coefficient of surrounding rock ($\mathcal{K}$) approaches to 1.0, it is more advantageous from vertical displacement, subsidence, and integrity of surface structures viewpoints. A smaller value of $\mathcal{K}$ appears more advantageous from a storage loss and cemented well annulus perspective. The surface above the salt dome can move upward with time when $\mathcal{K}$ is more than 1.0. When $\mathcal{K}$ is larger than 1.0, it is not better for the structural stability of caverns. When $\mathcal{K}$ is less than 1.0, $\mathcal{K}$ does not have effect on the structural stability of caverns. $\mathcal{K}$ is one of important parameters for the site selection and the design of SPR caverns. Therefore, data of in-suit stresses with depth in the surrounding rock should be acquired from the field if possible.

4.8. Effect of Cavern Size

To examine the effect of cavern size, the mesh was modified so that the cavern radius is 61 m (200 ft) instead of 30 m (100 ft) as used for the baseline. The spacing of caverns was maintained at 229 m (750 ft). The material properties for the salt dome, overburden, caprock, and surrounding rock are the same as those for the baseline. The model history and the thermal conditions are also the same as those for the baseline.

Based on an interpretation of the analyses results, a smaller cavern radius is more advantageous from storage loss, subsidence, integrity of surface structures, vertical strain above the roof of the cavern, and structural stability viewpoints. However, it is not better from a storage capacity per dome viewpoint. The optimum radius of cavern for each site should be analyzed on a case by case basis.

4.9. Depth Effect of Cavern

To examine the effect of cavern depth, the mesh was modified so that the top of the caverns are at depths of 305 m (1000 ft), 640 m (2100 ft), and 1219 m (4000 ft) instead of 762 m (2500 ft) for the baseline. The depth to the top of the salt dome is maintained at 610 m (2000 ft). However, the depth of salt dome top is decreased to 152 m (500 ft) when a cavern depth of 305 m (1000 ft) was modeled.

Table 5 lists the parameter values for the mesh used to examine the depth of cavern effect. The material properties for the salt dome, overburden, caprock, and surrounding rock are the same as those for the baseline case. The model history and the thermal conditions are also the same as those for the baseline except the cavern pressure for normal operating conditions because the wellhead pressure depends on the cavern depth. The wellhead pressures for the cavern depths of 305 m (1000 ft), 640 m (2100 ft), and 1219 m (4000 ft) are 2.55 MPa (370 psi), 5.36 MPa (777 psi), and 10.2 MPa (1480 psi), respectively, instead of 6.38 MPa (925 psi) for the baseline. The blue bold fonts in Table 5 indicate the different values from the baseline.

Table 5. The parameter values to examine the depth of cavern effect.

Parameter	Unit	d_C=1000	d_C=2100	Baseline d_C=2500	d_C=4000
Overburden Thickness (t_{OB})	ft	**100**	1600	1600	1600
Caprock Thickness (t_{CR})	ft	400	400	400	400
Depth of Salt dome top ($d_{SD} = t_{OB} + t_{CR}$)	ft	**500**	2000	2000	2000
Depth of Caverns (d_C)	ft	**1000**	**2100**	2500	**4000**
Wellhead Pressure for Normal Operating Conditions	psi	**370**	**777**	925	**1480**

From on an interpretation of the analyses results, a shallower depth for SPR caverns is more advantageous from storage loss, amount of subsidence, integrity of surface structures, and cemented well annulus viewpoints. On the other hand, a deeper depth for the caverns is more advantageous from both structural stability against tensile failure and dilatant damage viewpoints. It should be noted that operational efficiency decreases with increasing the depth of cavern. Therefore, the optimum depth should be sought for each site.

4.10. Effect of Number of Caverns

To examine the effect of the number of caverns, a symmetric 31-cavern field model was established so that readily deployed pie-slice models can be used. The 30-degree wedge model incorporates dome geometry appropriate for the site. Periodic workovers are simulated, but progressive leaches of the caverns for the drawdowns are not considered. Figure 5 shows a schematic of the 31-cavern field layout. Ring 5 is added to the symmetric 19-cavern field model in Figure 2. Again the same four baseline material blocks are used in the model: the overburden, caprock, salt dome, and surrounding lithologies. The diameter of the caverns is 61 m (200 ft), the distance between the caverns is 229 m (750 ft), the dome radius is 914 m (3000 ft), and the far-field boundary is 4572 m (15,000 ft) from the center of the dome as for the baseline case. The overburden

thickness, caprock thickness, depth of salt dome top, and depth of cavern top are kept the same as those for the baseline.

Based on an interpretation of the analyses results, a smaller number of caverns is more advantageous from a subsidence viewpoint. The number of caverns has little effect on the normalized storage loss and vertical strain above the roof of the cavern. The 31-cavern model shows a slight increase in radial surface strain. Caverns in the 19-cavern model are slightly more stable against tensile failure and dilatant damage than those in the 31-cavern model. The 31-cavern model has a larger storage capacity per dome and the impacts on SPR cavern integrity are small.

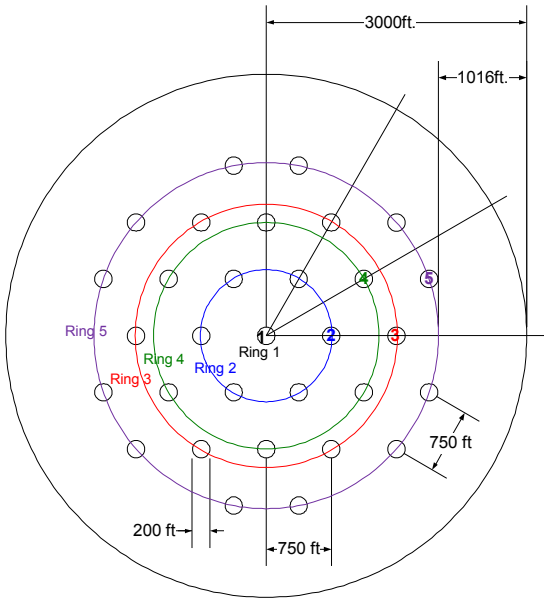

Figure 5. Schematic of 31-cavern field layout and cavern ring nomenclature.

5. CONCLUDING REMARKS

A sensitivity study was performed utilizing a three-dimensional finite element model to define allowable cavern field-sizes for a SPR salt dome. The effects of the parameters for creep rate, depth of salt dome top, dome size, caprock thickness, elastic modulus of caprock, elastic modulus of surrounding rock, lateral stress ratio of surrounding rock, cavern size, depth of cavern, and number of caverns were examined.

Table 6 lists the correlation between the parameters and their impact on the performance of the storage field. An upward pointing arrow (⬆) indicates a direct relationship between a parameter and an impact. For instance, the salt creep rate has a direct relationship on storage loss, i.e. a faster salt creep rate yields more storage loss of caverns with time. On the other hand, a downward pointing arrow (⬇) indicates an inverse relationship. If the symbol is red, it indicates a disadvantageous relationship for cavern field performance. For example, a faster salt creep rate yields greater storage loss, which is not good for the storage performance. A large symbol indicates a strong relationship. For example, the cavern depth has strong relationships with normalized storage loss, subsidence, possibility of tensile failure, possibility of dilatant damage, and operational efficiency. The cavern depth has relatively weak relationship with radial surface strain and vertical strains near the wellhead. The cavern depth has no relationship with storage capacity per dome. A leftward pointing arrow to 1 **(➡1)** indicates the lateral stress coefficient approaches to one.

We can obtain useful clues from this table for selecting a site and designing storage caverns by anticipating the degree in which the parameters impact the performance of the storage field. If we focus on the caprock thickness for example, a larger caprock thickness yields more storage loss and larger vertical strains near the wellhead, smaller subsidence, and an ignorable smaller radial surface strain. The caprock thickness has no relationship with the possibility of tensile failure, dilatant damage, and storage capacity of the dome.

This table can be utilized from the perspective of choosing a site based on design criteria. For instance, if the important issue in the design is the subsidence on the surface, the designer needs to consider a site with smaller salt creep rate, deeper depth of salt dome top, smaller radius of salt dome, larger thickness of caprock, larger elastic modulus of caprock and surrounding rock, a lateral stress coefficient of surrounding rock closer to one; and a cavern field design with smaller cavern radii, shallower depth of caverns, and smaller number of caverns. The more important factors for reducing the subsidence appear to be salt creep rate, elastic modulus of surrounding rock, lateral stress ratio of surrounding rock, cavern radius, and cavern depth. For another example, if a designer wants to develop a larger storage capacity per dome, he should consider more caverns in the dome rather than a larger cavern size. The table shows a larger radius of caverns yields more disadvantages than more caverns.

In general, a smaller salt creep rate, deeper depth of salt dome top, larger elastic modulus of the caprock and surrounding rock, and smaller cavern radius are better for the performance of a SPR cavern field.

↑: Direct relationship
-: No relationship
↓: Inverse relationship
Red: Disadvantageous
Blue: Advantageous

Table 6: Correlation Table

Parameter \ Impact on		Storage Loss	Subsidence	Radial Surface Strain	Vertical Strains near Wellhead	Possibility of Tensile Failure	Possibility of Dilatant Damage	Storage Capacity per Dome
Geologic parameters	Salt Creep Rate (↑)	↑	↑	↑	↑	- ↑ ††	↓ ↑ ‡‡	-
	Depth of Salt Dome Top (↑)	↓	↓	↓	↓	↓	↑	-
	Dome Radius(↑) Standoff Distance (↑)	↑	↑	↑	↓	↓	↑	-
	Caprock Thickness (↑)	↑	↓	↓	↑	-	-	-
	Elastic Modulus of Caprock (↑)	↓	↓	↓	↓	-	-	-
	Elastic Modulus of the Surrounding Rock (↑)	↑	↓	↓	↑	↓ - §§	↓ - ***	-
	Lateral Stress Ratio of Surrounding Rock (→1 †††)		↓	↓				-
	Lateral Stress Ratio of Surrounding Rock (↑)	↑			↑	↑	↑	-
Design parameters	Cavern Radius (↑)	↑	↑	↑	↑	↑	↑	↑
	Cavern Depth (↑)	↑	↑	↑	↑	↓	↓	-
	Number of Caverns (↑)	-	↑	↑	-	↑	↑	↑

††: increases after 17 years, ‡‡: increases after 12 years, §§: no relationship when E_{SR} > 20 GPa, ***: no relationship when E_{SR} > 10 GPa,
†††: approaches to 1

ACKNOWLEDGEMENT

This research is funded by SPR programs administered by the U.S. Department of Energy. Sandia is a multi program laboratory operated by Sandia Corporation, a Lockheed Martin Company, for the United States Department of Energy's National Nuclear Security Administration under Contract DE-AC04-94AL85000.

REFERENCES

1. Hoffman, E.L. and B.L. Ehgartner, 1996. Three Dimensional Finite Element Simulations of Room and Pillar Mines in Rock Salt, SAND96-0988C, *Presented at Second North American Rock Mechanics Symposium, Montreal, Quebec, June 9-12, 1996.*
2. Ehgartner, B.L. and Sobolik, S.R., 2002. *3-D Cavern Enlargement Analyses*, SAND2002-0526, Sandia National Laboratories, Albuquerque, NM 87185-0706.
3. Park, B.Y., B.L. Ehgartner, M.Y. Lee, and S.R. Sobolik, 2005. *Three Dimensional Simulation for Big Hill Strategic Petroleum Reserve (SPR)*, SAND2005-3216, Sandia National Laboratories, Albuquerque, NM.
4. Park, B.Y., B.L. Ehgartner, and M.Y. Lee, 2006. *Three Dimensional Simulation for Bayou Choctaw Strategic Petroleum Reserve (SPR)*, SAND2006-7589, Sandia National Laboratories, Albuquerque, NM.
5. Park, B.Y. and B.L. Ehgartner, 2008. *Expansion Analyses of Strategic Petroleum Reserve in Bayou Choctaw Salt Dome*, SAND2008-6408, Sandia National Laboratories, Albuquerque, NM.
6. Hoffman, E.L., 1992, *Investigation of Analysis Assumptions for SPR Calculations*, memo to J. K. Linn, Sandia National Laboratories, Albuquerque, New Mexico, February 7, 1992
7. Tammemagi, H.Y., M.C. Loken, J.D. Osnes, and R.A. Wagner, 1986. *A Compilation of Data for Thermomechanical Analyses of Four Potential Salt Repositories*, Technical Report, prepared for Office of Nuclear Waste Isolation Battelle Memorial Institute, 505 King Avenue Columbus, OH 43201-2693.
8. Lambe, T.W and R.V. Whitman, 1979. *Soil Mechanics*, SI Version, published by John Wiley & Sons.
9. Hoek E. and E.T. Brown, 1980. *Underground Excavations in Rock*, published by the Institution of Mining and Metallurgy, London
10. Munson, D.E., A.F. Fossum, and P.E. Senseny, 1989. *Advances in Resolution of Discrepancies between Predicted and Measured in Situ WIPP Room Closures*, SAND88-2948, Sandia National Laboratories, Albuquerque, New Mexico.

11. Krieg, R.D., 1984, *Reference Stratigraphy and Rock Properties for the Waste Isolation Pilot Plant (WIPP) Project*, SAND83-1908, Sandia National Laboratories, Albu-querque, NM 87185

12. Ballard, S. and Ehgartner, B.L., 2000, *CAVEMAN Version 3.0: System for SPR Cavern Pressure Analysis*, SAND2000-1751, Sandia National Laboratories, Albuquerque, NM 87185-0750.

13. Park, B.Y and B.L. Ehgartner, 2009. *Sensitivity of Storage Field Performance to Geologic and Cavern Design Parameters in Salt Domes*, SAND2009-1278, Sandia National Laboratories, Albuquerque, NM.